Inverse Problems

PAPER

Compton scatter tomography in annular domains

IOP Publishing Inverse Problems

Inverse Problems **35** (2019) 054005 (18pp) https://doi.org/10.1088/1361-6420/ab0b76

Compton scatter tomography in annular domains

T T Truong[1,3] **and M K Nguyen**[2]

[1] Laboratoire de Physique Théorique et Modélisation, Université de Cergy-Pontoise/CNRS UMR 8089, 2 rue Adolphe Chauvin, 95302 Cergy-Pontoise, France
[2] Laboratoire Équipes Traitement de l'Information et Systèmes (ETIS), Université de Cergy Pontoise/ENSEA/CNRS UMR 8051, 2 rue Adolphe Chauvin, 95302 Cergy-Pontoise, France

E-mail: truong@u-cergy.fr

Received 23 August 2018, revised 30 January 2019
Accepted for publication 28 February 2019
Published 2 May 2019

Abstract

Compton scatter tomography (CST) is an imaging process which reconstructs the electric charge density in a two-dimensional slice of an object. We describe a recent CST modality, introduced in 2010, designed to image an object from the data formed by the integrals of its electric charge density on a two parameter set of circular arcs in the plane, subtended by a rotating diameter of a fixed circle. Through a new approach based on a change of radial variables, introduced recently by Webber and Holman (2019 *Inverse Problems Imaging* **13** 231–61) in a three-dimensional function reconstruction problem, the CST Radon problems (interior and exterior to the fixed circle) can be mapped to the classical Radon transform. This relation provides not only an elegant solution to the CST reconstruction problems but also provides a link from the CST Radon problems on annular domains (interior and exterior to the fixed circle) to the well-known *exterior* classical Radon problem, for which results on function reconstruction have been fully worked out by Quinto. Such CST Radon problems on annular domains may arise, in practice, from restrictions near grazing or near grazing back scattering Compton scattering, as missing data tomographic problems, for which the proposed connection offers a concrete solution.

Keywords: generalized Radon transforms, Compton scatter tomography, imaging science integral geometry

(Some figures may appear in colour only in the online journal)

[3] Author to whom correspondence should be addressed.

1. Introduction

One way to image the inner parts of an object is to use penetrating (or ionizing) radiation to illuminate it and analyze the emerging radiation in view of reconstructing its internal structure. If non scattered radiation is recorded along the same incident radiation direction, this is known as computed tomography (CT), which reconstructs the object attenuation coefficient density via the inversion of the classical Radon transform (CRT). On the other hand, if scattered radiation is recorded at fixed scattered radiation energy, in a variety of directions, different from the incident direction—the great majority of this scattered radiation being from first order Compton scattering—, one speaks of Compton scatter tomography (or CST). In this case, it is the electric charge density which is reconstructed on the basis of its integrals on a dense family of two parameter circular arcs, connecting the radiation point source to the radiation detection site. The related mathematical problem will be called CST Radon problem and to each family of two parameter circular arcs corresponds a well defined CST modality.

So far there exits several CST modalities, for which the inversion formula of their corresponding CST Radon transforms can be established explicitly. The aim of this paper is to discuss a specific CST modality, which is proposed and solved in 2010 [2], under a new presentation and tackle one of its possible missing data problems, namely when scanning areas are limited to *annular* domains in the plane. Such a situation arises also recently for the Radon transform on circles centered on a fixed circle, which supports photo-acoustic tomography (PAT) and thermo-acoustic tomography (TAT), and for which the scanning areas are also limited to annular domains by Ambartsoumian *et al* in [3]. Missing (or limited) data problems are known in conventional tomography when the ranges of the two variables labeling the data are restricted, leading to indeterminacy in image reconstruction.

The paper is organized as follows. Section 2 reviews briefly the basic concept of Compton scatter tomography (CST) and its first modality suggested by Norton in 1994 [4]. Then the second CST modality is introduced in section 3. Then the two sub-modalities of CST-2 (interior and exterior, in sections 4 and 5) are presented under a new formulation, which is more transparent for the purpose of missing data problem. This is achieved by a change of radial variable, which is just the one introduced by Webber and Holman in the treatment of the so-called spindle transform [1] in three dimensions. This change of variable leads naturally and elegantly to a connection with the interior and the exterior classical Radon transforms, for which explicit standard inversion formulas are available. In section 6, we report new geometric properties of the interior and exterior CST-2 Radon transforms, which shall be relevant later for treating the missing data problem. Lastly, we come to the main section 7, in which the CST-2 Radon problem in annular domains is solved thanks to established results (mainly by Quinto) on the exterior classical Radon problem. A conclusion follows with opened perspectives for other CST modalities and objectives in studying and setting up computational algorithms for this CST-2 modality.

2. Compton scatter tomography and first Compton scatter tomography modality (CST-1)

CST has been known for decades, since Kondic suggested collecting Compton scattered data on isogonal circular arcs in 1978 for imaging purposes [5], a process based on the Compton formula expressing the scattered radiation energy $E(\omega)$ in terms of the scattering angle ω, for a review see e.g. [6]. However, it is only in 1994 that Norton came up with the first design of a CST scanner [4]. In this scanner, the object under study is 'scanned' by circular arcs having

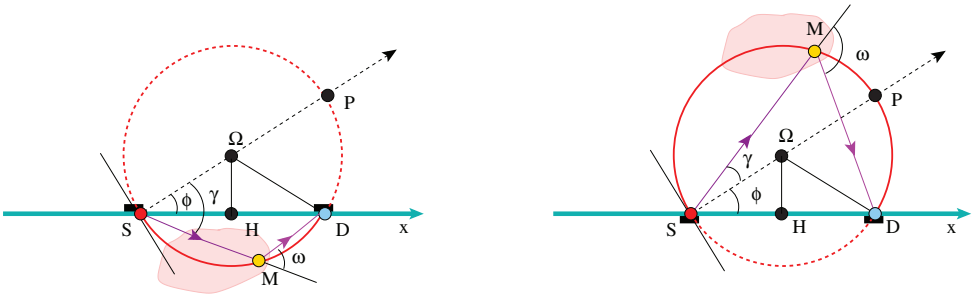

Figure 1. CST-1-Line. Scanning circular arcs $\widehat{SD}$ in lower half plane (left) and in upper half-plane (right).

one fixed end point S and another end point D moving on a line Δ passing through S and situated above Δ (see figure 1). This setup can be achieved by placing in the neighborhoods of S and D plate collimators parallel to the line Δ to confine all radiation to one side of Δ. At S is an isotropic monoenergetic point source of calibrated radiation emission flux density whereas at D is an energy sensitive point detector, registering scattered radiation from the object of energy $E(\omega)$. Inspection shows that the received scattered radiation flux density $\Phi_D(\omega)$ (assuming overwhelming dominance of first order scattering and no attenuation nor photometric effects) is of the form of an integral on $f(M)$, a function representing the object electric charge density at scattering site M:

$$\Phi_D(\omega) = K(\omega) \times \int_{M \in \widehat{SD}} \mathrm{d}l_M \; f(M), \tag{1}$$

where $K(\omega)$ is a factor containing the differential cross section of the Compton effect and some kinematic terms. The circular arc $\widehat{SD}$ is the locus of scattering sites M, subtending an inscribed angle $(\pi - \omega)$, which is constant when $E(\omega)$ is fixed. Thus in this context, the problem is to reconstruct $f(M)$ using the data $\Phi_D(\omega)/K(\omega)$, i.e. its integrals on this family of two parameter circular arcs. The solution to this problem has been discussed at length in many published works, see e.g. [4, 6].

The Norton CST scanner places the object to be imaged on one side of a line Δ (horizontal line in figure 1). This is convenient for large objects. However it does not lend itself to the setting of a compact radiation shielding protecting human operating personnel because of its 'open space' concept. We shall denote this modality by CST-1-Line[4].

In 2010, we have introduced a new CST-2 modality [2, 6], which is conceived for efficient use in scanning large objects (outer scanning) as well as small objects (inner scanning), with adequate compact radiation shielding for the protection of operating personnel.

3. Second Compton scatter tomography modality (CST-2)

Historically, interior (resp. exterior) CST-2 Radon transform was introduced in [2]. We have then followed Cormack's procedure, which consists in inverting a Chebyshev integral equation linking angular Fourier components of the unknown function (called 'circular components') to those of the measured CST-2 Radon data. Soon after Palamodov, recognizing that the Cormack's type of reconstruction formula is not stable, has managed, using his equivalence

[4] Recently, a CST-1-Circle modality has been introduced and discussed in [8, 9].

of CST-2 Radon transform with the Minkowski–Funk transform [7], to derive an alternative reconstruction formula which is stable for function circular components. In this section, we give a change of radial variable which directly converts the CST-2 Radon transform into the classical Radon transform. Then using the stable form of the inversion formula of the classical Radon transform, which is widely known, we derive a stable inversion formula for our CST-2 Radon transform. In the meantime, Cormack had also realized that his inversion approach did lead to instabilities and has proposed a way out by taking into account the so-called 'consistency conditions' on the Radon data [15]. In this way, stable inverse formulas for Radon transforms on his α (resp. β) curves, (see [16]) have been established. This is how he recovered a stable inversion formula for the classical Radon transform, which is in fact a Radon transform on $\alpha = 1$ curves (or straight lines). Hence a direct short-cut to stable inversion formulas for CST-2 Radon transform can be deduced easily.

Furthermore, it will be shown that the proposed change of variable also converts the CST-2 Radon transforms in annular scanning domains into the *exterior* classical Radon transform for which well established inversion results due to Quinto exist. Consequently, the CST-2 Radon problems in annular domains are automatically and elegantly solved thanks to these mappings. Had we attempted to formulate these CST-2 Radon problems in annular domains by conventional integral Chebyshev transform, we would be facing with modified integration limits (see for example (equation (7)) of [3]), which render the usual inversion impossible. In this situation, perhaps the technique of converting this problem into a Volterra's problem [3] may work, but at this point this has not been done.

Our change of variable is just the one of Webber–Holman in [1], which is designed to map their *spindle* Radon transform (a three-dimensional version of our CST-2 Radon transform [2]) to Radon transform on circular cylinders in $\mathbb{R}^3$.

Let $f(M)$ be a non negative real function representing the electric charge density of an object with compact support inside (resp. outside) a disk $\mathscr{D}(O,p)$, of center O (taken as the coordinate system origin) and of radius p. Its boundary is a circle $\Gamma(O,p) = \partial\mathscr{D}(O,p)$. The concept of CST-2 is presented as follows. An isotropic mono-energetic point source S is located at some position on $\Gamma(O,p)$, whereas an energy sensitive point detector D is diametrically positioned on $\Gamma(O,p)$, as shown in figure 2. At both S and D are plate collimators to confine radiation to a half space delimited by the line SD. Again (under the assumption of overwhelming dominance of first order scattering) original radiation coming from S is scattered by the object electric charge at some site M and the scattered flux density registered at D is also given by equation (1). If site D records only scattered radiation of energy $E(\omega)$, the locus of scattering sites M is a circular arc $\widehat{SD}$ with end points on a rotating diameter of $\Gamma(O,p)$, subtending an inscribed angle $(\pi - \omega)$. So such a scanning arc is characterized by ω and ϕ, the polar angle of the scanning arc axis of symmetry perpendicular to SD. It can be seen that there are two classes of such scanning arcs: those which are inside $\mathscr{D}(O,p)$ (when $0 < \omega < \pi/2$) and those which are outside $\mathscr{D}(O,p)$ (when $\pi/2 < \omega < \pi$). This distinguishes an interior CST-2 Radon problem from its exterior CST-2 counterpart. The problem posed by these two CCT-2 modalities is the reconstruction of $f(M)$ (inside and outside $\mathscr{D}(O,p)$) from its integrals on corresponding families of such scanning arcs.

4. Interior CST-2 Radon problem

We consider first the interior problem for which the support of $f(M)$ is contained inside $\mathscr{D}(O,p)$. The corresponding Radon problem is formulated in the following proposition:

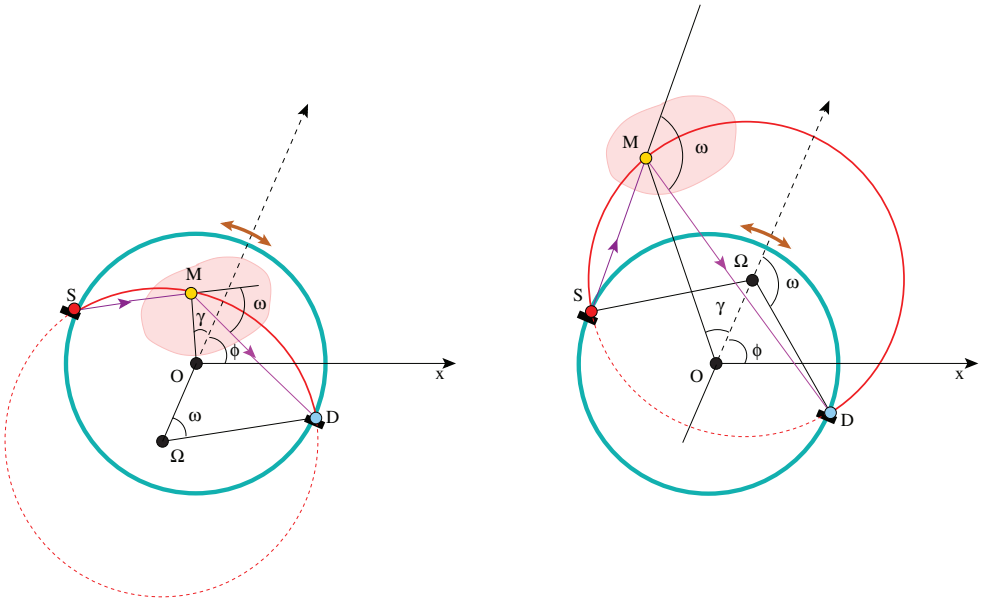

Figure 2. CST-2. Interior problem with $0 < \omega < \pi/2$ (left) and exterior problem with $\pi/2 < \omega < \pi$ (right).

Proposition 4.1. *Let $f(r_i, \theta_i)$ be an integrable function of compact support in $\mathscr{D}(O,p)$ in polar coordinates (r_i, θ_i). The interior CST-2 Radon transform maps $f(r_i, \theta_i)$ to $\widehat{f}_i(\tau, \phi)$ according to*

$$\widehat{f}_i(\tau,\phi) = \frac{\sqrt{\tau^2+1}}{\tau} \int_{p(\sqrt{\tau^2+1}-\tau)}^{p} \frac{\mathrm{d}r_i}{\sqrt{1-\frac{1}{4\tau^2}\left(\frac{p}{r_i}-\frac{r_i}{p}\right)^2}} \{f(r_i, \gamma_i+\phi) + f(r_i, -\gamma_i+\phi)\}, \tag{2}$$

where $0 < \tau < \infty$, $0 < \phi < 2\pi$ and

$$\gamma_i = \cos^{-1} \frac{1}{2\tau}\left(\frac{p}{r_i} - \frac{r_i}{p}\right). \tag{3}$$

The parameter τ is related to the physical Compton scattering angle ω by $\tau = \cot\omega$ with $0 < \omega < \pi/2$.

Proof. Consider figure 2 with polar coordinates centered at O. An interior scanning circle for $0 < \omega < \pi/2$ has a center at Ω on the mediator line of the source-detector line SD below it. Then $O\Omega = p\,\cot\omega$. Its radius is $\Omega D = p/\sin\omega$. Now a running point M on this circle is given by its polar coordinates (r_i, θ_i), with $OM = r_i$ and $\theta_i = \gamma_i + \phi$, where $\gamma = \gamma_i$ and ϕ are given in figure 2. In triangle $OM\Omega$, we have the cosine identity

$$M\Omega^2 = O\Omega^2 + OM^2 - 2\,O\Omega\,OM\,\cos\widehat{\Omega OM}.$$

Since $M\Omega = \Omega D = p/\sin\omega$ and $\widehat{\Omega OM} = (\pi - \gamma_i)$, we get the interior scanning circle equation

$$\cos\gamma_i = \frac{1}{2\tau}\left(\frac{p}{r_i} - \frac{r_i}{p}\right), \tag{4}$$

which is equivalent to equation (3), see [2]. □

Then by solving r_i in terms of γ_i, one gets the equation of a CST-2 interior scanning circular arc (parameterized by (τ, ϕ))

$$r_i(\gamma_i) = p\left(\sqrt{\tau^2\cos^2\gamma_i + 1} - \tau\cos\gamma_i\right), \tag{5}$$

where $\gamma_i = (\theta_i - \phi)$ with $(-\pi/2 < \gamma_i < \pi/2)$. As pointed out, τ is related to the scattering angle by $\tau = \cot\omega$ with $(0 < \omega < \pi/2)$. We observe that $r_i(\gamma_i)$ is an increasing function of γ_i, and $p(\sqrt{\tau^2+1} - \tau) < r_i(\gamma_i) < p$. Then straightforwardly one has

$$\mathrm{d}r_i = r_i\,\mathrm{d}\gamma_i\ \frac{\tau\sin\gamma_i}{\sqrt{\tau^2\cos^2\gamma_i + 1}}. \tag{6}$$

The scanning arc integration element $\mathrm{d}l_i = \sqrt{\mathrm{d}r_i^2 + r_i^2\mathrm{d}\gamma_i^2}$ can be obtained from equation (5), via the computation of $\mathrm{d}r_i$ using equation (5), (see equation (8) of [2]) as

$$\mathrm{d}l_i = \sqrt{\tau^2+1}\ \frac{r_i(\gamma_i)\,\mathrm{d}\gamma_i}{\sqrt{\tau^2\cos^2\gamma_i + 1}}. \tag{7}$$

The integral of $f(r_i, \theta_i)$ on this interior CST-2 scanning arc is

$$\widehat{f}_i(\tau,\phi) = \sqrt{\tau^2+1}\int_{-\pi/2}^{\pi/2}\frac{r_i(\gamma_i)\,\mathrm{d}\gamma_i}{\sqrt{\tau^2\cos^2\gamma_i+1}} f\left(r_i(\gamma_i), \gamma_i + \phi\right). \tag{8}$$

Since we have a $\gamma_i \to -\gamma_i$ symmetry in $\mathrm{d}l_i$, equation (8) can be rewritten as

$$\widehat{f}_i(\tau,\phi) = \sqrt{\tau^2+1}\int_{0}^{\pi/2}\frac{r_i(\gamma_i)\,\mathrm{d}\gamma_i}{\sqrt{\tau^2\cos^2\gamma_i+1}}\left\{f\left(r_i(\gamma_i), \gamma_i + \phi\right) + f\left(r_i(\gamma_i), -\gamma_i + \phi\right)\right\}. \tag{9}$$

Now by using equation (6), we can get an alternative expression of $\mathrm{d}l_i$ in terms of $\mathrm{d}r_i$:

$$\mathrm{d}l_i = \frac{\sqrt{\tau^2+1}}{\tau}\ \frac{\mathrm{d}r_i}{\sqrt{1 - \frac{1}{4\tau^2\left(\frac{p}{r_i} - \frac{r_i}{p}\right)^2}}}. \tag{10}$$

Then equation (9) becomes equation (2).

4.1. Connection to the full plane classical Radon transform

We now show that, under a radial change of variable, $\widehat{f}_i(\tau,\phi)$ can be expressed as a line integral for a transformed input function. Such a conversion is analogous to geometric inversion which connects the classical Radon transform (on lines)[5] to the Radon transform on circles passing through a fixed point [10–12]. The change of variable considered here is the one proposed by Webber–Holman to treat the so-called *spindle* transform in three dimensions [1].

[5] Following [10], we use the denomination of classical Radon transform to speak of the original integral transform introduced by Radon in 1917.

Proposition 4.2. *Under the assumptions of proposition 4.1 and the change of variable* $r_i \rightarrow \rho_i$, *given by*

$$r_i = p\left(\sqrt{\frac{p^2}{\rho_i^2}+1} - \frac{p}{\rho_i}\right), \tag{11}$$

the integral of $f(r,\theta)$ *on an interior CST-2 scanning arc becomes an integral on a line with parameters* (s,ϕ) *(or of equation* $s = \rho_i \cos(\theta_i - \phi)$*)*

$$\widehat{f}_i(\tau,\phi) = \frac{\sqrt{\tau^2+1}}{\tau} \int_s^\infty \frac{\mathrm{d}\rho_i}{\sqrt{1-\frac{s^2}{\rho_i^2}}} \{h(\rho_i, \gamma_i + \phi) + h(\rho_i, -\gamma_i + \phi)\}, \tag{12}$$

for the function

$$h(\rho_i,\theta_i) = \frac{p^2}{\rho_i^2} \frac{\left(\sqrt{\frac{p^2}{\rho_i^2}+1} - \frac{p}{\rho_i}\right)}{\sqrt{\frac{p^2}{\rho_i^2}+1}} f\left(p\left(\sqrt{\frac{p^2}{\rho_i^2}+1} - \frac{p}{\rho_i}\right), \theta_i\right), \tag{13}$$

where $s = p/\tau$ *with* $0 < s < \infty$ *(since* $0 < \tau < \infty$*) and* $0 < \phi < 2\pi$ *and*

$$\gamma_i = \cos^{-1}\left(\frac{s}{\rho_i}\right).$$

Equation (12) has the standard form of the classical Radon transform of $h(\rho_i,\theta_i)$ expressed in radial variable ρ_i, see e.g. [13], page 4, equation (1.9).

Remark 4.3. The mapping (11) may look peculiar but it has a simple geometric interpretation. Since $O\Omega = p\tau$ and $s = p/\tau$, s being the distance from the origin to the straight line, with unit normal vector $\mathbf{n} = (\cos\phi, \sin\phi)$ and transform of the interior scanning circular arc, we conclude that $O\Omega \cdot s = p^2$. As $s > 0$, we may consider a point Ω^* symmetric of Ω with respect to O such that $O\Omega^* = p\tau$ also. Then one may view the line as the geometric polar line of Ω^* with respect to the fixed circle $\Gamma(O,p)$. Generalized change of variables of this type have been found for other CST modalities in [32]. Their geometric aspects and consequences have been discussed in [17].

Remark 4.4. The proof of injectivity has been already given in [2]. The problem may be reformulated as a Volterra type inversion problem as in [3]. But this has not been done yet. On the other hand, we choose to consider CST-2 stability properties as deduced from well established stability properties of the associated classical Radon transform obtained by the previous change of variable.

Proof. To prove this statement, we proceed to rewrite $\widehat{f}_i(\tau,\phi)$ in terms of the new variable ρ_i. From equation (11), we get

$$\mathrm{d}r_i = \frac{p^2}{\rho_i^2}\left(\sqrt{\frac{p^2}{\rho_i^2}+1} - \frac{p}{\rho}\right) \frac{\mathrm{d}\rho_i}{\sqrt{\frac{p^2}{\rho_i^2}+1}}, \tag{14}$$

and using the fact that

$$\frac{1}{2\tau}\left(\frac{p}{r_i}-\frac{r_i}{p}\right)=\frac{s}{\rho_i}, \tag{15}$$

we end up with equations (12) and (13). □

4.2. Inversion of the interior CST-2 Radon transform

As the interior CST-2 Radon problem is now connected to the full plane classical Radon problem, the classical Radon transform has a reconstruction formula, given e.g. by equation (21) of [14, 15]. Hence we have

Proposition 4.5. *Under the assumptions of proposition 4.1, the reconstruction of $f(r_i,\theta_i)$ inside the disk $\mathscr{D}(O,p)$ with complete data is given by*

$$f(r_i,\theta_i)=-\frac{1}{2\pi^2}\,\frac{2p^2(p^2+r_i^2)}{(p^2-r_i^2)^2}\int_0^{2\pi}\mathrm{d}\phi\int_0^{\infty}\mathrm{d}\tau\,\frac{1}{\frac{p}{\tau}-\frac{2p^2}{p^2-r_i^2}r_i\cos(\theta_i-\phi)}\,\frac{\partial}{\partial\tau}\left(\frac{\tau\widehat{f}_i(\tau,\phi)}{\sqrt{\tau^2+1}}\right), \tag{16}$$

where $(r_i,\theta_i)\in\mathscr{D}(O,p)$.

Proof. To obtain the result of equation (16), we start from the reconstruction formula of the classical Radon transform for the intermediate function $h(\rho_i,\theta)$, given e.g. in [14, 15], which is

$$h(\rho_i,\theta_i)=-\frac{1}{2\pi^2}\int_0^{2\pi}\mathrm{d}\phi\int_0^{\infty}\mathrm{d}s\,\frac{1}{s-\rho_i\cos(\theta_i-\phi)}\,\frac{\partial}{\partial s}\left(\frac{\tau}{\sqrt{\tau^2+1}}\,\widehat{f}_i(\tau,\phi)\right). \tag{17}$$

Then we use the definition of $h(\rho_i,\theta)$ given by equation (13) and replace ρ_i by its expression in terms of r_i

$$\rho_i=r_i\,\frac{2p^2}{p^2-r_i^2}. \tag{18}$$

Finally using $s=p/\tau$, by reexpressing s-differentiation in terms of τ-differentiation and replacing $\mathrm{d}s$ by $\mathrm{d}\tau$, we obtain the desired result of equation (16). □

5. Exterior CST-2 Radon problem

The exterior CST-2 Radon problem bears many similarities with the interior CST-2 Radon problem. However we choose to present the derivation of its inversion along the line of the previous section for clarity and to emphasize its complementarity to the previous one. The exterior CST-2 Radon problem is formulated in the following proposition

Proposition 5.1. *Let $f(r_i,\theta_i)$ be an integrable function of compact support outside the disk $\mathscr{D}(O,p)$ in $\mathbb{R}^2$. The exterior CST-2 Radon transform maps $f(r_e,\theta_e)$ to $\widehat{f}_e(\tau,\phi)$ according to*

$$\widehat{f}_e(\tau,\phi) = \frac{\sqrt{\tau^2+1}}{\tau}\int_p^{p(\sqrt{\tau^2+1}-\tau)} \frac{\mathrm{d}r_e}{\sqrt{1-\frac{1}{4\tau^2}\left(\frac{r_e}{p}-\frac{p}{r_e}\right)^2}}\{f(r_e,\gamma_e+\phi)+f(r_e,-\gamma_e+\phi)\}, \tag{19}$$

where $0<\tau<\infty$, $0<\phi<2\pi$ *and*

$$\gamma_e = \cos^{-1}\frac{1}{2\tau}\left(\frac{r_e}{p}-\frac{p}{r_e}\right). \tag{20}$$

Proof. In polar coordinates centered at O (see figure 2), where $M=(r_e,\theta_e)$, the equation of a CST-2 exterior scanning circular arc is obtained in a similar way as in the case of CST-2 interior scanning circular arc

$$r_e(\gamma_e) = p\left(\sqrt{\tau^2\cos^2\gamma_e+1}+\tau\cos\gamma_e\right), \tag{21}$$

where $\gamma_e=(\theta_e-\phi)$ with $(-\pi/2<\gamma_e<\pi/2)$. The parameter τ is now connected to the scattering angle $(\pi/2<\omega<\pi)$ by $\tau=-\cot\omega$. We observe that $r_e(\gamma_e)$ is a decreasing function of γ_e, and $p<r_e(\gamma_e)<p(\sqrt{\tau^2+1}+\tau)$. The scanning arc integration element $\mathrm{d}l_e$ can be obtained from equation (21) (analogously to the interior problem via the computation of $\mathrm{d}r_e$) as

$$\mathrm{d}l_e = \sqrt{\tau^2+1}\,\frac{r_e(\gamma_e)\,\mathrm{d}\gamma_e}{\sqrt{\tau^2\cos^2\gamma_i+1}}. \tag{22}$$

The integral of $f(r_e,\theta_e)$ on this exterior CST-2 scanning arc is

$$\widehat{f}_e(\tau,\phi) = \sqrt{\tau^2+1}\int_{-\pi/2}^{\pi/2}\frac{r_e(\gamma_e)\,\mathrm{d}\gamma_e}{\sqrt{\tau^2\cos^2\gamma_e+1}}f\left(r_e(\gamma_e),\gamma_e+\phi\right). \tag{23}$$

Since we have a $\gamma_e\ \rightarrow\ -\gamma_e$ symmetry in $\mathrm{d}l_e$, equation (23) can be rewritten as

$$\widehat{f}_e(\tau,\phi) = \sqrt{\tau^2+1}\int_0^{\pi/2}\frac{r_e(\gamma_e)\,\mathrm{d}\gamma_e}{\sqrt{\tau^2\cos^2\gamma_e+1}}\{f\left(r_e(\gamma_e),\gamma_e+\phi\right)+f\left(r_e(\gamma_e),-\gamma_e+\phi\right)\}. \tag{24}$$

Now switch to r_e variable,

$$\mathrm{d}l_e = \frac{\sqrt{\tau^2+1}}{\tau}\,\frac{\mathrm{d}r_e}{\sqrt{1-\frac{1}{4\tau^2\left(\frac{r_e}{p}-\frac{p}{r_e}\right)^2}}}, \tag{25}$$

then equation (24) becomes equation (19). □

5.1. Connection to the full plane classical Radon transform

We now show that, under an analogous radial change of variable, $\widehat{f}_e(\tau,\phi)$ can be expressed as a line integral for a transformed input function. By definition,

Proposition 5.2. *Under the assumptions of proposition 5.1 and the change of variable* $r_e\ \rightarrow\ \rho_e$, *given by*

$$r_e = p\left(\sqrt{\frac{p^2}{\rho_e^2}+1}+\frac{p}{\rho_e}\right), \tag{26}$$

the integral of $f(r_e,\theta_e)$ *on an exterior CST-2 scanning arc becomes an integral on a line with parameters* (s,ϕ)*:*

$$\widehat{f}_e(\tau,\phi) = \frac{\sqrt{\tau^2+1}}{\tau}\int_s^\infty \frac{\mathrm{d}\rho_e}{\sqrt{1-\frac{s^2}{\rho_e^2}}}\{h(\rho_e,\gamma_e+\phi)+h(\rho_e,-\gamma_e+\phi)\}, \tag{27}$$

for the function

$$h(\rho_e,\theta_e) = \frac{p^2}{\rho_e^2}\frac{\left(\sqrt{\frac{p^2}{\rho_e^2}+1}+\frac{p}{\rho_e}\right)}{\sqrt{\frac{p^2}{\rho_e^2}+1}} f\left(p\left(\sqrt{\frac{p^2}{\rho_e^2}+1}+\frac{p}{\rho_e}\right),\theta_e\right), \tag{28}$$

where $s = p/\tau$ *with* $0<s<\infty$ *(since* $0<\tau<\infty$*)and* $0<\phi<2\pi$*, and*

$$\gamma_e = (\theta_e-\phi) = \cos^{-1}\left(\frac{s}{\rho_e}\right).$$

Equation (27) has the standard form of the classical Radon transform of $h(\rho_e,\theta_e)$ expressed in radial variable ρ_e, see e.g. [13], page 4, equation (1.9). This change of variable has not appear before as it has emerged from earlier work on this subject [17] and now sheds new light on this problem.

Proof. To prove this statement, we proceed to rewrite $\widehat{f}_e(\tau,\phi)$ in terms of the new variable ρ_e. From equation (11), we get

$$\mathrm{d}r_e = \frac{p^2}{\rho_e^2}\left(\sqrt{\frac{p^2}{\rho_e^2}+1}-\frac{p}{\rho_e}\right)\frac{\mathrm{d}\rho_e}{\sqrt{\frac{p^2}{\rho_e^2}+1}}, \tag{29}$$

and using the fact that

$$\frac{1}{2\tau}\left(\frac{r_e}{p}-\frac{p}{r_e}\right) = \frac{s}{\rho_e}, \tag{30}$$

we end up with equations (27) and (28). □

5.2. Inversion of the exterior CST-2 Radon transform

As the interior CST-2 Radon problem is now connected to the full plane classical Radon problem, the classical Radon transform has a reconstruction formula, given e.g. by equation (21) of [15]. Hence we have

Proposition 5.3. *Under the assumptions of proposition 5.1, the reconstruction of* $f(r_e,\theta_e)$ *outside the disk* $\mathscr{D}(O,p)$ *with complete data is given by*

$$f(r_e,\theta_e) = -\frac{1}{2\pi^2}\,\frac{2p^2(r_e^2+p^2)}{(r_e^2-p^2)^2}\int_0^{2\pi} \mathrm{d}\phi \int_0^{\infty} \mathrm{d}\tau\, \frac{1}{\frac{p}{\tau} - \frac{2p^2}{r_e^2-p^2} r_e \cos(\theta_e-\phi)}\,\frac{\partial}{\partial\tau}\left(\frac{\tau \widehat{f}_i(\tau,\phi)}{\sqrt{\tau^2+1}}\right), \tag{31}$$

where $r_e > p$ *and* $0 < \theta < 2\pi$.

Proof. To obtain the result of equation (31), we start from the reconstruction formula of the classical Radon transform for the intermediate function $h(\rho_e,\theta_e)$, given in [15], which is

$$h(\rho_e,\theta_e) = -\frac{1}{2\pi^2}\int_0^{2\pi} \mathrm{d}\phi \int_0^{\infty} \mathrm{d}s\, \frac{1}{s-\rho_e\cos(\theta_e-\phi)}\,\frac{\partial}{\partial s}\left(\frac{\tau}{\sqrt{\tau^2+1}}\,\widehat{f}_e(\tau,\phi)\right). \tag{32}$$

Then we use the definition of $h(\rho_e,\theta_e)$ given e.g. by equation (28) and replace ρ_e by its expression in terms of r_e:

$$\rho_e = r_e\,\frac{2p^2}{r_e^2-p^2}. \tag{33}$$

Finally using $s = p/\tau$, by reexpressing s-differentiation in terms of τ-differentiation and replacing $\mathrm{d}s$ by $\mathrm{d}\tau$, we obtain the desired result of equation (31). □

Remark 5.4. We may view the change of variable $r \to \rho$ as a map from type-2 Compton scatter tomography (CST-2) to an apparent computed tomography (CT), whereby the real electric charge density $f(r,\theta)$ is mapped to an apparent attenuation coefficient density $h(\rho,\theta)$.

6. Geometric connection between interior and exterior CST-2 Radon transforms

In this section, we point out a remarkable connection between interior and exterior CST-2 Radon transforms, discussed in sections 4 and 5 above: they are linked by geometric inversion in the circle $\Gamma(O,p)$[6]. This is described by the following statements.

Proposition 6.1. *For the same angle* $\gamma_i = \gamma_e = \gamma$, *we have* $r_i(\gamma)\cdot r_e(\gamma) = p^2$ *and* $\rho_i = \rho_e = \rho$.

Proof. Use equations (5) and (21) to show that $r_i(\gamma)\cdot r_e(\gamma) = p^2$. Next use equations (18) and (33) to show that $\rho_i = \rho_e = \rho$. This explains why both interior and exterior arcs are mapped to the *same* line $s = \rho_{i,e}\ \cos(\theta_{i,e}-\phi)$, which is just the polar line of the center of the exterior arc with respect to circle $\Gamma(O,p)$ [17]. □

Remark 6.2. One may think of the mapping of the exterior (resp. interior) CST-2 Radon transform to the classical Radon transform as the product of geometric inversion in the circle $\Gamma(O,p)$ and of the mapping of the interior (resp. exterior) CST-2 Radon transform to the classical Radon transform.

[6] We use the denomination of *geometric inversion* to avoid confusion with inversion of an integral operator, as in [12].

Proposition 6.3. *Let $f(r_i,\theta_i)$ be a non-negative integrable function in the disk $\mathscr{D}(O,p)$ and $\widehat{f}_i(\tau,\phi)$ its interior CST-2 Radon transform. Then $\widehat{f}_i(\tau,\phi)$ can be expressed as the exterior CST-2 Radon transform of $g(r_e,\theta_e)$, given by*

$$g(r_e,\theta_e)=\frac{p^2}{r_e^2}\,f\left(\frac{p^2}{r_e}\theta_e\right), \tag{34}$$

where $r_e>p$ and $(0<\theta_e=\theta_i<2\pi)$. The converse, in which the indices (i) and (e) are exchanged, is also true, provided that one replaces 'inside $\mathscr{D}(O,p)$' by 'outside $\mathscr{D}(O,p)$'.

Proof. We start from the expression of $\widehat{f}_i(\tau,\phi)$ as an integral over r_i, given by equation (2). Then insert the geometric inverse relation $r_i=p^2/r_e$ and calculate $\mathrm{d}r_i$ in terms of $\mathrm{d}r_e$ to re-express this equation in terms of r_e

$$\widehat{f}_i(\tau,\phi)=\frac{\sqrt{\tau^2+1}}{\tau}\int_p^{p(\sqrt{\tau^2+1}+\tau)}\frac{\mathrm{d}r_e}{\sqrt{1-\frac{1}{4\tau^2}\left(\frac{r_e}{p}-\frac{p}{r_e}\right)^2}}\,\frac{p^2}{r_e^2}\left\{f(\frac{p^2}{r_e},\gamma_e+\phi)+f(\frac{p^2}{r_e},-\gamma_e+\phi)\right\}, \tag{35}$$

where $0<\tau<\infty$, $0<\phi<2\pi$ and $\gamma_e=\gamma_i$. Thus this is the exterior CST-2 Radon transform of $g(r_e,\theta_e)$ as defined above. □

Had we started out with $\widehat{f}_e(\tau,\phi)$, the proof can be repeated by exchanging the indices $(i)\rightleftarrows(e)$ and changing the integration bounds to $(p(\sqrt{1+\tau^2}-\tau)\to p)$.

Remark 6.4. Lastly, for imaging the full plane, it is necessary to use both (albeit separately) interior and exterior CST-2 scanning. It is amusing to compare this double CST-2 scanning (at supplementary scattering angles) to the double scanning (also at supplementary scattering angles) advocated for CST-1-line Radon transform in [18], which was shown to be equivalent to the scanning by the so-called V-line by application of geometric inversion.

7. The CST-2 Radon problem in an annular domain and its inversion

Theoretical reconstruction of electric charge density in CST requires complete data, as in conventional CT. In practice restrictions on measurements have led to the problem of missing (or limited data). Since the CST-2 data is labeled by two parameters (τ,ϕ), there will be two possible classes of missing data related either to restricted τ or to restricted ϕ. Here, assuming that *SD* can move freely around its center *O*, we shall be concerned only with restrictions on τ.

7.1. Origin of the problem—mapping to the exterior classical Radon problem

As known, CST relies on the measurement of scattered radiation flux at given scattered energy. This is done by radiation detector crystals, which have bounded energy detection ranges. More specifically,

- for interior CST-2, one may not be able to pick up data for grazing scattering angle $\omega\sim 0(\omega>0)$, so that the effective range of Compton scattering angle is restricted to $(0<\omega_{\min}<\omega<\pi/2)$. Consequently the τ-range is now $0<\tau<\tau_{\min}$ since $\tau=\cot\omega$, or $s_{\min}<s<\infty$, since $s=p/\tau$. The scanning arcs are located inside an circular annulus

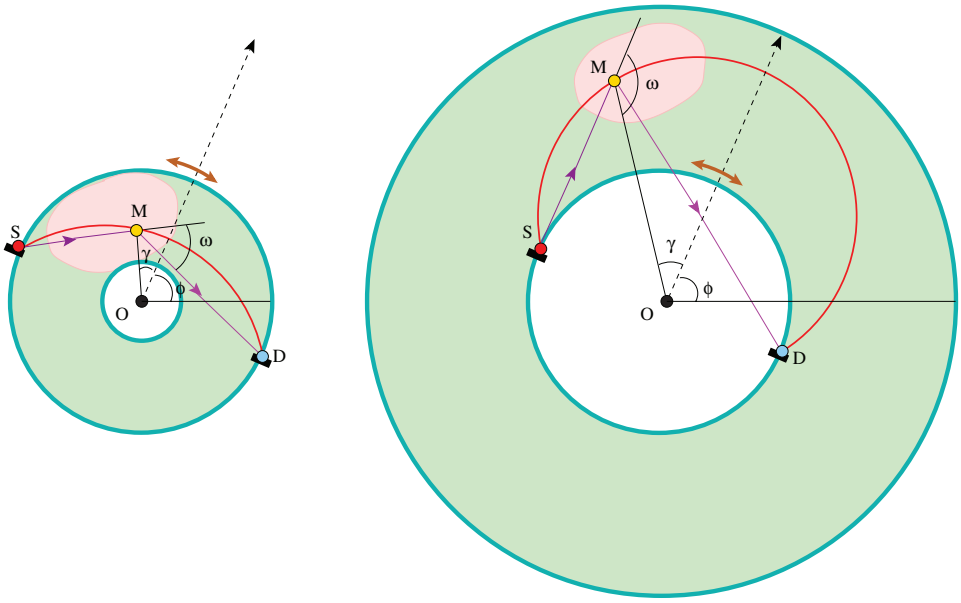

Figure 3. Annular interior (left) and exterior (right) CST-2.

$\mathscr{A}(p(\sqrt{1+\tau^2}-\tau),p)$, between interior radius $p(\sqrt{1+\tau^2}-\tau)$ and exterior radius p, see left image of figure 3. Following the radial mapping $r_i \rightarrow \rho_i$, as no restriction is imposed on ϕ, one gets, instead of the full plane classical Radon problem, now the so-called *exterior* classical Radon problem, since the new scanning lines in (ρ_i,θ_i) space do not intersect the disk $\mathscr{D}(O,s_{\min})$,

- for exterior CST-2, one may not be able to pick up data for grazing scattering angle $\omega \sim \pi, (\omega < \pi)$, so that the effective range of Compton scattering angle is restricted to $\pi/2 < \omega < \omega_{\max}$. Consequently the τ-range is now $0 < \tau < \tau_{\max}$ since $\tau = -\cot\omega$, or $s_{\max} < s < \infty$, since $s = p/\tau$. The scanning arcs are located inside an circular annulus $\mathscr{A}(p,p(\sqrt{1+\tau^2}+\tau))$, between interior radius p and exterior radius $p(\sqrt{1+\tau^2}+\tau)$, see right image of figure 3. Following the radial mapping $r_e \rightarrow \rho_e$, as no restriction is imposed on ϕ, one gets, instead of the full plane classical Radon problem, now the so-called *exterior* classical Radon problem, since the new scanning lines in (ρ_i,θ_i) space do not intersect the disk $\mathscr{D}(O,s_{\max})$.

Note that the two annular domains $\mathscr{A}(p(\sqrt{1+\tau^2}-\tau),p)$ and $\mathscr{A}(p,p(\sqrt{1+\tau^2}+\tau))$ are morphologically identical. Function reconstruction problem for the interior annular domain can be transferred to that of the exterior domain or vice versa by relabeling the variables from one to the other case. Moreover if one chooses $s_{\min}\cdot s_{\max} = p^2$, then geometric inversion in the circle $\Gamma(O,p)$ connects the interior annulus $\mathscr{A}(p(\sqrt{1+\tau^2}-\tau),p)$ to the exterior annulus $\mathscr{A}(p,p(\sqrt{1+\tau^2}+\tau))$, see right image of figure 4. So one would need to consider only one CST-2 Radon problem on annular domain.

The question is now how to use the results on the exterior Radon problem to build up a function reconstruction procedure for CST-2 Radon transform on annular domains.

However, if the compact support of $f(r,\theta)$ is *strictly* inside $\mathscr{A}(p(\sqrt{1+\tau^2}-\tau),p)$ (or inside $\mathscr{A}(p,p(\sqrt{1+\tau^2}+\tau))$), then the inversion is given by formula (16) (or by formula

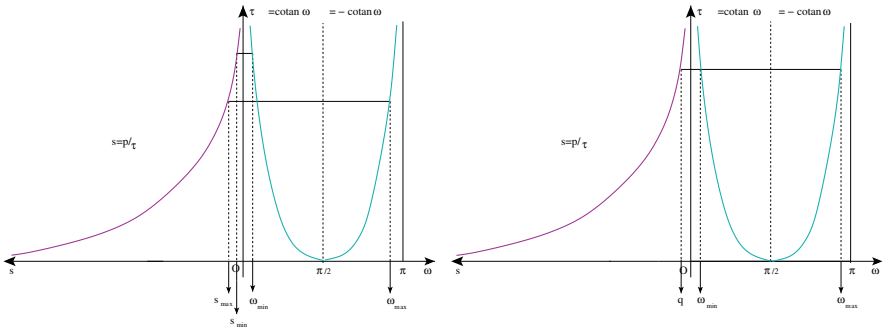

Figure 4. CST-2-Parameters values s (red curve) and ω (blue curve).

(31)), as in the case of available full data. But in general this is not the case and we have to resort to using the reconstruction in exterior classical Radon problem, which is most comprehensively worked out by Quinto in [11, 25–27]. We shall follow the exposition of his method in describing the reconstruction algorithm.

7.2. The exterior classical Radon problem associated to interior/exterior CST-2 Radon problems

In this subsection, we review the status of the exterior Radon problem, now associated to both interior and exterior CST-2 Radon problems. We shall denote $(\rho_{i,e}, \theta_{i,e})$ by (ρ, θ) and $(s_{\min,\max})$ by q, see right image of figure 4. In principle, the exterior classical Radon problem is soluble for integrable functions with compact support, which is the case of all physical densities of interest, as asserted by general theorems [19, 20] and the so-called 'hole theorem' of Cormack [21, 22]. However the reconstruction via the 'hole theorem' is unstable. A stable version of it was obtained later [15, 22], which agrees with the one found by Perry [23]. The first investigation on the exterior classical Radon transform is due to Perry [24], who established the singular value decomposition (SVD) of the classical Radon integral operator including its null space. Perry concluded that no complete function reconstruction can be achieved. But later on, Quinto, in a series of papers, produces, for smooth functions with compact support, a reconstruction algorithm which effectively inverts the exterior classical Radon transform in [11, 25, 26, 28]. We shall follow Quinto's approach for our purposes.

(a) The exterior Radon transform concerns intermediate functions $h(\rho, \theta)$, defined on $\mathscr{E} = \{(\rho, \theta) : (q < \rho < \infty) \cup (0 < \theta < 2\pi)\}$, the exterior of a disk $\mathscr{D}(O, q)$ in $\mathbb{R}^2$, which are assumed to be square integrable, i.e. $h(\rho, \theta) \in \mathscr{L}^2(\mathscr{E})$ with respect to the integration measure

$$\frac{\rho}{q}\sqrt{1-\frac{q^2}{\rho^2}}\,\rho\,\mathrm{d}\theta\,\mathrm{d}\rho. \tag{36}$$

This classical exterior Radon transform maps $h(\rho, \theta)$ to $\widehat{h}(s, \phi)$, which is defined on $\mathscr{E}' = \{(s, \phi) : (q < s < \infty) \cup (0 < \phi < 2\pi)\}$, the exterior of a disk $\mathscr{D}'(O, q)$ in $\mathbb{R}^2$. It is also assumed that $\widehat{h}(s, \phi) \in \mathscr{L}^2(\mathscr{E}')$, with respect to the integration measure

$$\frac{q}{s}\,\mathrm{d}\phi\,\mathrm{d}s. \tag{37}$$

Note that the physical dimension of $\widehat{h}(s,\phi)$ is equal to the physical dimension of $h(\rho,\theta)$ times a length, since $h(\rho,\theta)$ is integrated over a straight line.

(b) There exists, in $\mathscr{L}^2(\mathscr{E})$, the following orthonormal basis, for $m = \mathbb{N}$ and $l \in \mathbb{Z}$:

$$h_{lm}(\rho,\theta) = \frac{q^2}{\rho^2}\, Q_m\left(-\frac{1}{2},\frac{1}{2},\frac{q^2}{\rho^2}\right)\, \mathrm{e}^{\mathrm{i}l\theta}, \quad \text{for } l \text{ even},$$
$$h_{lm}(\rho,\theta) = \frac{q^3}{\rho^3}\, Q_m\left(\frac{1}{2},\frac{1}{2},\frac{q^2}{\rho^2}\right)\, \mathrm{e}^{\mathrm{i}l\theta}, \quad \text{for } l \text{ odd}, \tag{38}$$

where $Q_m(\alpha,\beta,t) = (2^{1+\alpha+\beta}/h_m^{(\beta,\alpha)})\, P_m^{(\alpha,\beta)}(2t-1)$, $P_m^{(\alpha,\beta)}(2t-1)$ is the standard (α,β) Jacobi polynomial [29] and $h_m^{(\beta,\alpha)}$ is a numerical factor given by equation (4.3.3) of [30].

On the other hand, in $\mathscr{L}^2(\mathscr{E}')$,

$$\widehat{h}_{lm}(s,\phi) = \frac{q^{l+2}}{s^{l+1}}\, Q_m\left(l,0,\frac{q^2}{s^2}\right)\, \mathrm{e}^{\mathrm{i}l\phi}, \tag{39}$$

form a basis in $\mathscr{L}^2(\mathscr{E}')$, for $m = \mathbb{N}$ and $l \in \mathbb{Z}$.

(c) The exterior classical Radon transform maps $h_{lm}(\rho,\theta)$ to $\widehat{h}_{lm}(s,\phi)$ according to

$$h_{lm}(\rho,\theta) \to 0, \qquad \text{for} \quad m < \left[\frac{|l|}{2}\right],$$
$$\to \sqrt{\frac{2\pi}{|l|+2m'+1}}\, \widehat{h}_{lm}(s,\phi) \qquad \text{for} \quad m > \left[\frac{|l|}{2}\right], \tag{40}$$

where $m' = (m - [|l|/2])$ and $[t]$ is the largest integer at most equal to t.

(d) In [25], Quinto has designed a numerical inversion algorithm to uniquely recover $h(\rho,\theta)$, of compact support and made up of two components $h(\rho,\theta) = h_R(\rho,\theta) + h_N(\rho,\theta)$, where $h_N(\rho,\theta)$ is the so-called null component since its classical Radon transform is zero and $h_R(\rho,\theta)$ is the 'regular' component. His procedure consists of the following steps:

- Decompose the data $\widehat{h}(s,\phi)$ on the basis formed by the $\widehat{h}_{lm}(s,\phi)$ as

$$\widehat{h}(s,\phi) = \sum_{l,m} c_{l,m}\, \widehat{h}_{lm}(s,\phi). \tag{41}$$

- Recover the 'regular' part $h_R(\rho,\theta)$ of the unknown function $h(\rho,\theta)$, as

$$h_R(\rho,\theta) = \sum_{l,m} \frac{c_{l,m}}{\sqrt{\frac{2\pi}{|l|+2m'+1}}}\, h_{lm}(\rho,\theta). \tag{42}$$

- The next step is to determine $h_N(\rho,\theta)$, by determining its circular component $h_{N,l}(\rho)$, which is the angular Fourier component of $h_N(\rho,\theta)$ in

$$h_N(\rho,\theta) = \sum_{l\in\mathbb{Z}} h_{N,l}(\rho)\, \mathrm{e}^{\mathrm{i}l\theta}. \tag{43}$$

Quinto, in [25–27] has shown that $h_{N,l}(\rho)$ is a polynomial in $1/\rho$ of the same parity as l, of degree at most $|l|$ and with lowest order term in $1/\rho$ of degree at least equal to two. Therefore the first three circular components $h_{N,0}(\rho)$ and $h_{N,\pm1}(\rho)$ are zero. As $h(\rho,\theta)$ is of compact support, we know that there exist $K > q$ such that for all $\rho > K$ we have $h_{N,l}(\rho) = -h_{R,l}(\rho)$.

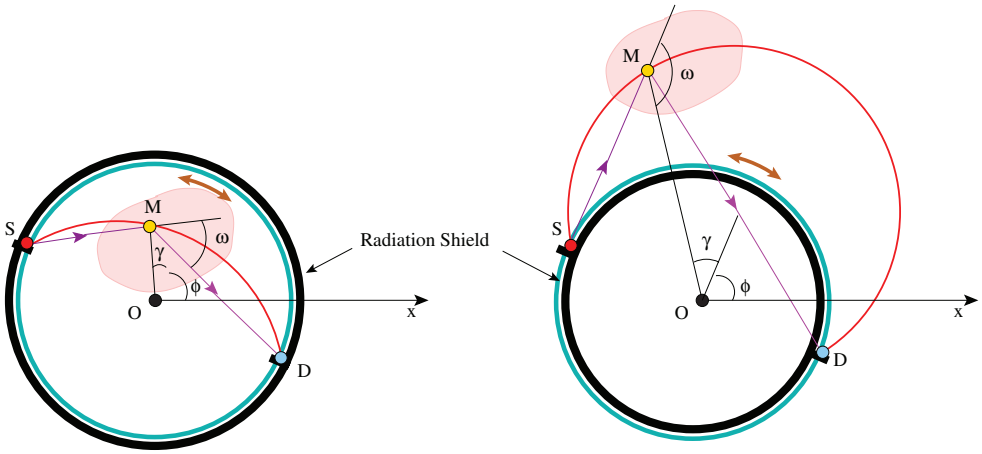

Figure 5. Interior (left) and exterior (right) CST-2 shielding.

This condition fixes uniquely $h_{N,l}(\rho)$ for $\rho > q$, because it is a polynomial in $1/\rho$. This completes the determination of $h(\rho, \theta)$.

7.3. Application to the inversion of the CST-2 Radon transform in annular domain from an interior (resp. exterior) CST-2 Radon problem

We are now in a position to reconstruct fully the interior CST-2 Radon transform in an annular domain. Once $h(\rho_i, \theta_i)$ (resp. $h(\rho_e, \theta_e)$) is obtained from the previous algorithm, we invert equation (13) (resp. equation (28)) using also the expression of ρ_i (resp. of ρ_e) in equation (18) (resp. equation (33)) to get the sought functions

$$f(r_i, \theta_i) = \frac{2p^2(p^2 + r_i^2)}{(p^2 - r_i)^2}\, h\left(r_i \frac{2p^2}{(p^2 - r_i^2)}\right), \tag{44}$$

$$f(r_e, \theta_e) = \frac{2p^2(p^2 + r_e^2)}{(r_e^2 - p^2)^2}\, h\left(r_e \frac{2p^2}{(r_e^2 - p^2)}\right), \tag{45}$$

which is the set objective of this work.

8. Conclusion and perspectives

In this paper, we have presented a particular modality of Compton scatter tomography, called CST-2 and introduced in 2010, under a new approach and studied one of its missing data problem, which amounts to restrict the scanning area to an annular domain instead of the interior (or exterior) of a disk. We have shown that this problem, through an appropriate change of radial variable is reduced to the *exterior* classical Radon transform. The function reconstructive procedure in the case of the *exterior* classical Radon transform, worked out by Quinto, has been applied to reconstruct the unknown function of compact support in the two CST-2 sub-modalities.

Interior CST-2 has potentially more imaging applications (nuclear medicine, non-destructive testing and evaluation, etc) as exterior CST-2, which by, its structure is meant for imaging

large two-dimensional areas, e.g. two-dimensional search for land mines using Compton effect. In both operating modes, there is a need to protect operating personnel from strayed radiation. As already mentioned, CST-2 lends itself nicely to the installation of a circular shield as pictured in figure 5. For interior CST-2 scanning, the operator is positioned *outside* the circular shield, while the object under study lies inside the circle $\Gamma(O,p)$. For exterior CST-2 scanning, the operator is placed *inside* the circular shield since the exterior of the shield is subjected to scanning radiation from the moving source S. In this case, strong radiation sources are expected to be used in order to have sensible measurement results. Note that this modality is more practical for scanning large areas than Norton's CST-1-line modality.

We have not touched upon the problem of numerical inversion algorithm, which is quite formidable and reserve it for a future publication with a serious theoretical study of finite discretization of the data as well as of the inversion algorithm, along the lines of Marr's work [31].

An extension of this work to what we may call CST-3 [32], in which scanning arcs have end points on the boundary circle $\Gamma(O,p)$ but remain orthogonal to $\Gamma(O,p)$. In this case, there exists also radial mappings which converts the interior and exterior problems into the same *interior* classical Radon problem, allowing elegant inversion formulas to be derived. Then the problem of missing data, due to limited energy range of radiation detectors, will be reduced to the CST-3 problem in annular domains. We hope to be able to deal with more new CST modalities through generalizations of the radial change of variables in order to be able to map these problems to the well-known classical Radon transform, for which a rich host of properties and techniques are readily available.

Acknowledgments

We thank referee 1 for bringing [1] and its contents to our attention. Referee 2 also made many constructive suggestions and we are grateful to both of them for their critical remarks which have contributed to improve the presentation of this paper.

ORCID iDs

T T Truong https://orcid.org/0000-0002-7019-773X
M K Nguyen https://orcid.org/0000-0003-1192-0980

References

[1] Webber J and Holman S 2019 Microlocal analysis of a spindle transform *Inverse Problems Imaging* **13** 231–61
[2] Nguyen M K and Truong T T 2010 Inversion of a new circular arc Radon transform for Compton scattering tomography *Inverse Problems* **26** 065005
[3] Ambartsoumian G, Gouia-Zarrad R and Lewis M A 2010 Inversion of the circular Radon transform on an annulus *Inverse Problems* **26** 105015
[4] Norton S J 1994 Compton scattering tomography *J. Appl. Phys.* **76** 2007–15
[5] Kondic N N 1978 Density field determination by an external stationary radiation source using a kernel technique *Measurements in Polyphase Flows* (*Papers of the ASME Winter Annual Meeting (San Francisco, CA, USA, 10–15 December 1978)*) ed D E Stock (ASME) pp 37–51
[6] Truong T T and Nguyen M K 2012 Recent developments on Compton scatter tomography: theory and numerical simulations, in *Numerical Simulation—from Theory to Industry* ed M Andriychuk (Rijeka: InTech) pp 101–28

[7] Palamodov V P 2011 An analytic reconstruction for the Compton scattering tomography in a plane *Inverse Problems* **27** 125004
[8] Rigaud G 2017 Compton scattering tomography: feature reconstruction and rotation-free modality *SIAM J. Imaging Sci.* **10** 2217–49
[9] Tarpau C and Nguyen M K 2018 A novel modality of Compton Scattering Tomography: image formation and reconstruction *Image Processing and Computer Vision Conf. (Las Vegas, USA, July 30–August 02 2018)*
[10] Quinto E T 1982 Null spaces and ranges for the clasical and spherical Radon transforms *J. Math. Anal. Appl.* **90** 408–20
[11] Quinto E T 1983 Singular value decompositions and inversion methods for the exterior Radon transform and a spherical transform *J. Math. Anal. Appl.* **95** 437–48
[12] Yagle A E 1992 Inversion of spherical means using geometric inversion and Radon transforms *Inverse Problems* **8** 949–64
[13] Perry R M 1985 Reconstructing a function by circular harmonic analysis of its Radon transform *National Center for Atmospheric Research Technical Note* NCAR/TN-255+STR
[14] Nievergelt Y 2006 Elementary inversion of Radon's transform *SIAM—Rev.* **28** 79–84
[15] Cormack A M 1984 Radon's problem—old and new *SIAM—AMS Proc.* 14 33–9
[16] Cormack A M 1981 The Radon transform on a family of curves in the plane *Proc. Am. Math. Soc.* 83 325–30
[17] Truong T T 2014 On geometric aspects of circular arcs Radon transforms for Compton scatter tomography *Eurasian J. Math. Comput. Appl.* **2** 40–69
[18] Truong T T and Nguyen M K 2015 New properties of the V-line Radon transform and their imaging applications *J. Phys. A: Math. Theor.* **48** 405204
[19] Helgason S 1965 The Radon transform on Euclidean spaces, compact two-point homogeneous spaces and Grassmann manifolds *Acta Math.* **113** 153–80
[20] Ludwig D 1966 The Radon transform on Euclidean space *Commun. Pure Appl. Math.* **19** 49–81
[21] Cormack A M 1963 Representation of a function by its line integrals, with some radiological applications *J. Appl. Phys.* **34** 2722–7
[22] Natterer F 1983 Exploiting the ranges of Radon transforms in tomography *Numerical Treatment of Inverse Problems in Differential and Integral Equations* ed P Deufhard *et al* (Boston, MA: Birkhäuser) pp 290–303
[23] Perry R M 1975 Reconstruction of a function by circular harmonic analysis of its Radon transform *Opt. Soc. Am.* (*Digest of Topical Meeting on Image Processing for 2D and 3D Reconstruction (Washington)*)
[24] Perry R M 1977 On reconstructing a function on the exterior of a disk from its Radon transform *J. Math. Anal. Appl.* **59** 324–41
[25] Quinto E T 1988 Tomographic reconstructions from incomplete data—numerical inversion of the exterior Radon transform *Inverse Problems* **4** 867–76
[26] Quinto E T 1991 Computed tomography and rockets *Mathematical Methods in Tomography* (*Lecture Notes in Mathematics* vol 1497) ed G T Herman *et al* (Berlin: Springer) pp 261–8
[27] Quinto E T 1998 Exterior and limited-angle tomography in non-destructive evaluation *Inverse Problems* **14** 339–53
[28] Quinto E T 2007 Local algorithms in exterior tomography *J. Comput. Appl. Math.* **199** 141–8
[29] Magnus W, Oberhettinger F and Soni R P 1966 *Formulas and Theorems for the Special Functions of Mathematical Physics* 3rd edn (Berlin: Springer)
[30] Szegö G 1939 *Orthogonal Polynomials* (Providence, RI: American Mathematical Society)
[31] Marr R B 1974 On the reconstruction of a function on a circular domain from a sampling of its line integrals *J. Math. Anal. Appl.* **45** 357–74
[32] Truong T T and Nguyen M K 2011 Radon transforms on generalized Cormack's curves and a new Compton scatter tomography modality *Inverse Problems* **27** 125001